

QCD factorization at fixed $Q^2(1-x)$ *

PAUL HOYER

Department of Physics and Helsinki Institute of Physics
 POB 64, FIN-00014 University of Helsinki, Finland

Amplitudes of hard *exclusive* processes such as $\gamma^*(Q^2)N \rightarrow \gamma Y$, where $Y = N$ (DVCS) or any other state with a limited mass ($M_Y^2 \ll Q^2$), factorize into a hard subprocess amplitude and a target (transition) GPD. The corresponding *inclusive* cross section, summed over all states Y of a given (limited) mass, is then given by the discontinuity of a forward multiparton distribution. An application to the Drell-Yan process $\pi^+ N \rightarrow \gamma^*(x_F, Q^2) + Y$ allows to explain the observed longitudinal polarization of the virtual photon at high x_F .

PACS numbers: 12.38.Bx, 13.88.+e

1. The inclusive – exclusive connection

The optical theorem expresses the cross section of deep inelastic lepton scattering $eN \rightarrow eX$ as a discontinuity of the forward $\gamma^*(q)N(p)$ amplitude. In the Bjorken limit where the photon virtuality $-q^2 = Q^2 \rightarrow \infty$ at fixed $x_B = Q^2/2p \cdot q$ this amplitude factorizes into the $\gamma^*(q)q(x_B p) \rightarrow \gamma^*(q)q(x_B p)$ hard subprocess amplitude and a target parton distribution (PDF, Fig. 1(a)).

The factorization property can be readily understood intuitively. The invariant mass M_X of the inclusive system grows with Q ,

$$M_X^2 = (p + q)^2 = m_N^2 + \frac{1}{x_B}(1 - x_B)Q^2 \rightarrow \infty \quad \text{in the Bj limit} \quad (1)$$

The virtual photon transfers its large momentum to the struck quark which hadronizes nearly independently of the target spectators. Factorization does not hold at low hadronic mass M_X (*i.e.*, for $x_B \rightarrow 1$) due to coherence effects

* Talk at Epiphany meeting in commemoration of Jan Kwieciński, Krakow, January 2009. Based on work done in collaboration with Matti Järvinen and Samu Kurki [1].

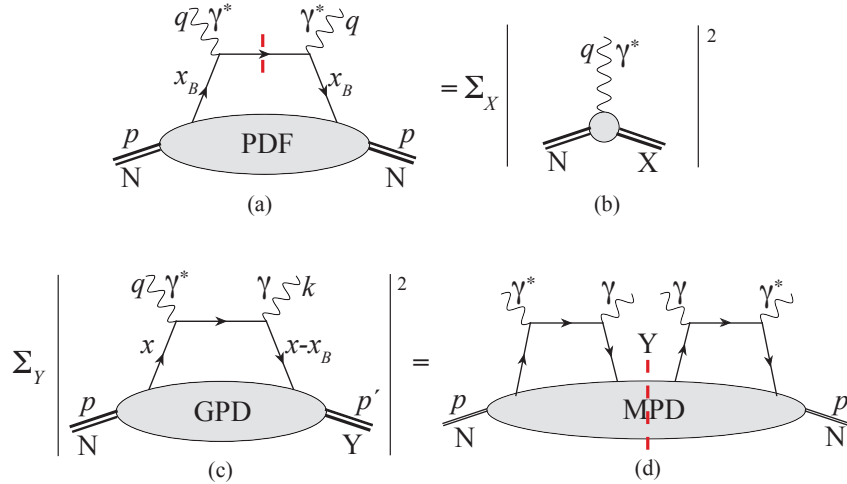


Fig. 1. The discontinuity of the forward $\gamma^*N \rightarrow \gamma^*N$ amplitude (a) equals the DIS cross section (b). The PDF is real, hence the discontinuity is obtained by cutting only the struck quark (dashed line). Analogously, the sum over Y of the squares of the $\gamma^*N \rightarrow \gamma Y$ amplitudes (c) is given by the discontinuity of the forward multiparton distribution (d).

between the struck quark and the spectators. The optical theorem itself is exact and may be applied even for $X = N$ ($x_B = 1$), in which case the discontinuity of the forward $\gamma^*N \rightarrow \gamma^*N$ amplitude measures the square of the elastic form factor in Fig. 1(b). Intriguing similarities – Bloom-Gilman duality [2] – are nevertheless observed between the nucleon elastic and transition form factors on the one hand and the factorized, high M_X^2 DIS cross section on the other. This may contain clues to the dynamics of the exclusive form factors [3].

Instead of the discontinuity of the forward $\gamma^*N \rightarrow \gamma^*N$ amplitude we may consider the non-forward $\gamma^*N \rightarrow \gamma Y$ amplitude measured in Deeply Virtual Compton Scattering (DVCS). As indicated in Fig. 1(c) this amplitude factorizes similarly to DIS in the Bjorken limit. The large momentum imparted to the struck quark is carried away by the final photon and the quark then fuses with the target spectators into a low-mass system Y , often taken to be the nucleon itself ($Y = N$). The soft target dynamics is described by a Generalized Parton Distribution (GPD) [4] which is real and in the forward limit reduces to the PDF of Fig. 1(a). An integral over x of the GPD gives the elastic (or transition, $N \rightarrow Y$) nucleon form factors. These form factors could not be obtained from the PDF of Fig. 1(a) since DIS factorization breaks down at fixed M_X , *i.e.*, for $x_B \rightarrow 1$ with $(1 - x_B)Q^2$ fixed.

The GPD factorization shown in Fig. 1(c) works in the Bj limit for any final state Y whose mass is small compared to the total CM energy given in (1), $M_Y^2 \ll M_X^2$. M_Y is kinematically constrained by the momentum k carried away by the real photon. We may parametrize the external momenta using $p = (p^+, p^-, \mathbf{p}_\perp)$ notation ($p^\pm = p^0 \pm p^3$) as

$$\begin{aligned} q &= (-Q, Q, \mathbf{0}_\perp) \\ p &= (Q/x_B, m_N^2 x_B/Q, \mathbf{0}_\perp) \\ k &= (k_\perp^2/(x_F Q), x_F Q, \mathbf{k}_\perp) \end{aligned} \quad (2)$$

where $k_\perp \ll Q$ is the transverse momentum of the final photon and the Feynman $x_F = k^-/q^-$. This gives

$$M_Y^2 = (p + q - k)^2 = \frac{1 - x_B}{x_B} (1 - x_F) Q^2 \left[1 + \mathcal{O}\left(\frac{1}{Q^2}\right) \right] \quad (3)$$

GPD factorization works at any fixed M_Y , *i.e.*, keeping $(1 - x_F)Q^2$ fixed. We may then use completeness in the system Y to relate the *inclusive* DVCS process $\gamma^* N \rightarrow \gamma Y$ to the discontinuity of the forward multiparton distribution (MPD) shown in Fig. 1(d).

2. The BB limit

The method illustrated above for DVCS may be applied to many other processes. We were motivated [1] particularly by the data on the Drell-Yan reaction $\pi^+ N \rightarrow \gamma^* Y$, which may be viewed as a time reversed version of DVCS, with the real photon replaced by the pion. A dramatic change in the polarization of the virtual photon, from transverse to longitudinal, was observed [5] at high x_F . According to an early analysis by Berger and Brodsky [6] this signals the emergence of a dynamics in which both valence quarks of the pion scatter coherently, transferring nearly all their momentum ($x_F \rightarrow 1$) and helicity ($\lambda = 0$) to the virtual photon. Thus we refer to the limit considered here as the

$$\text{BB limit : } Q^2 \rightarrow \infty \quad \text{at fixed } Q^2(1 - x) \quad (4)$$

Here x may refer either to the momentum fraction x_F of particle in the final state (such as the real photon in DVCS) or to a parton momentum fraction in a hadron (such as a valence quark in the pion of the Drell-Yan process) and Q is the hard scale (a large virtuality or transverse momentum).

The life-time of a hadron Fock state is inversely proportional to ΔE , the energy difference between the hadron and its Fock state. At high hadron momentum p ,

$$2p\Delta E \simeq m_h^2 - \sum_i \frac{p_{i\perp}^2 + m_i^2}{x_i} \quad (5)$$

where the x_i are the momentum fractions and $p_{i\perp}$ the transverse momenta of the partons in the Fock state. In the BB limit (4) a parton with $x \rightarrow 1$ and $p_{\perp}^2 \sim Q^2$ thus contributes to ΔE similarly as the partons carrying $1-x \sim \Lambda_{QCD}^2/Q^2$ and $p_{\perp}^2 \sim \Lambda_{QCD}^2$. Hence soft interactions of the partons with low x are coherent with, and influence, the hard interactions of the large x parton.

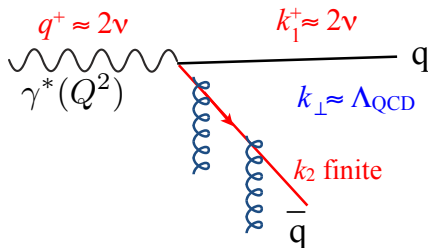


Fig. 2. Light-Front time x^+ development of DIS when the virtual photon momentum is along the positive z -axis. The photon fluctuates into an asymmetric $q\bar{q}$ pair where the quark carries nearly all the momentum whereas the antiquark has finite momentum in the target rest frame even as $q^+ \rightarrow \infty$. Soft scattering of the antiquark in the target (indicated by the vertical gluons) triggers the hard DIS process.

A good example of such coherence is provided by DIS itself, viewed in the “target rest frame” ($q^+ \simeq 2\nu$). The Light-Front (LF) time (x^+) development is sketched in Fig. 2. The virtual photon splits asymmetrically into a quark pair, $\gamma^* \rightarrow q(z) + \bar{q}(1-z)$, with the quark carrying nearly all the momentum ($k_q^+ \simeq 2\nu$) while the antiquark momentum $k_{\bar{q}}^+ = 2\nu(1-z) \sim \Lambda_{QCD}$ is fixed as $\nu \rightarrow \infty$. Since $\nu \propto Q^2$ the $q\bar{q}$ Fock state of the virtual photon illustrates the BB limit (4). In light-cone gauge ($A^- = 0$) only the \bar{q} scatters (softly) in the target, which sets the quark on-shell and thus “causes” the hard DIS interaction. The hard γ^* and soft \bar{q} interactions are coherent due to their commensurate lifetimes: $x_{\bar{q}}^+ \sim 1/k_{\bar{q}}^-$ and $x_{\gamma^*}^+ \sim 2\nu/Q^2 = 1/mx_B$ are both finite. In the usual “handbag” picture of DIS the antiquark in Fig. 2 is viewed as the target quark which is struck by the γ^* , and its soft target interactions are part of the bound state dynamics.

3. Drell-Yan in the BB limit

The dynamics of $\pi^+ N \rightarrow \gamma^*(x_F) + Y$ for

$$x_F = \frac{q^-}{k^-} \rightarrow 1 \quad (6)$$

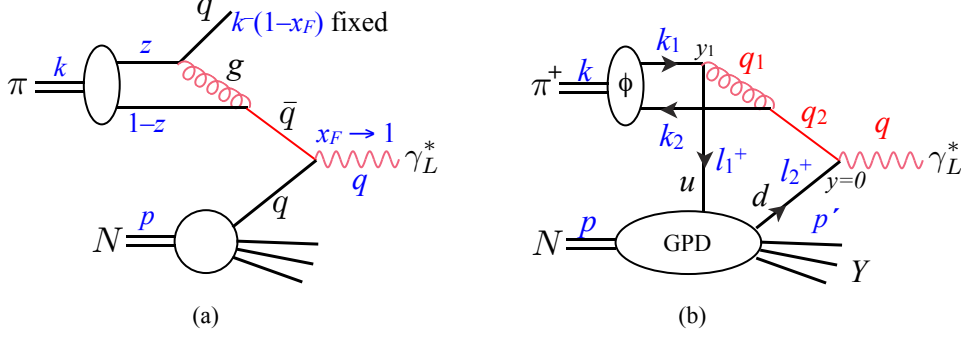


Fig. 3. (a) For the photon to carry nearly all the momentum of the pion ($x_F \rightarrow 1$) the momentum zk carried by the quark q is transferred to the antiquark \bar{q} via gluon g exchange, with both the g and the \bar{q} acquiring virtualities of $\mathcal{O}(Q^2)$. (b) The gluon emission leaves the quark with a finite momentum $\ell_1^- = k^-(1 - x_F)$ in the target rest frame. The interactions of the quark within the target are coherent with the hard subprocess and described by a target (transition) GPD, which involves an integral over ℓ_1^- and $\ell_{1\perp}$.

as discussed by Berger and Brodsky [6] is shown in Fig. 3(a). The virtualities of the annihilating \bar{q} and the exchanged g are of $\mathcal{O}(Q^2)$, hence the hard subprocess involves both quarks in the pion. This makes a longitudinal polarization of the photon possible, in contrast to the transverse polarization resulting from the $q\bar{q} \rightarrow \gamma^*$ process with quarks of low virtuality.

As in the Bjorken limit we take $q^2 = Q^2 \rightarrow \infty$ with

$$x_B = \frac{q^+}{p^+} = \frac{Q^2}{2q \cdot p} = \frac{Q^2}{s} \quad \text{fixed} \quad (7)$$

where we used (6) to set $q^- \simeq k^-$. The inclusive mass

$$M_Y^2 = (k + p - q)^2 \simeq (1 - x_B) [s(1 - x_F) + m_N^2] - q_\perp^2 \quad (8)$$

being fixed in the BB limit (4) the momentum $k^-(1 - x_F)$ of the “stopped” quark in the pion must be finite in the target rest frame. This quark remains coherent with the hard subprocess and its soft target interactions cannot be ignored, in analogy to the antiquark in the DIS process of Fig. 2. Thus we arrive at Fig. 3(b), which represents the amplitude for a specific state Y . (The inclusive DY cross section will be obtained below by squaring this amplitude and summing over Y .)

As the pion momentum in the target rest frame $k^- \rightarrow \infty$ and the relative transverse momentum \mathbf{k}_\perp of its quark constituents stays limited we may

approximate the valence quark momenta as

$$\begin{aligned} k_1 &= (0^+, zk^-, \mathbf{k}_\perp) \\ k_2 &= (0^+, (1-z)k^-, -\mathbf{k}_\perp) \end{aligned} \quad (9)$$

The gluon $g(q_1)$ which transfers the u -quark momentum onto the \bar{d} is highly virtual,

$$q_1^2 \simeq -zk^-\ell_1^+ \rightarrow -\infty \quad (10)$$

which means that the pion Fock state is transversally compact and described by the pion distribution amplitude $\phi_\pi(z)$. Similarly

$$\begin{aligned} q_2^2 &\simeq -k^-\ell_1^+ \rightarrow -\infty \\ q_1^- &\simeq zq_2^- \simeq zk^- \rightarrow \infty \end{aligned} \quad (11)$$

Hence the target vertices $\bar{u}(y_1)$ and $d(y=0)$ are separated by correspondingly short distances

$$\begin{aligned} y_{1\perp} &= \mathcal{O}(1/Q) \rightarrow 0 \\ y_1^+ &= \mathcal{O}(1/k^-) \rightarrow 0 \end{aligned} \quad (12)$$

On the other hand, the coherence length along the light-cone remains finite,

$$y_1^- = \mathcal{O}(1/\ell_1^+) \quad (13)$$

Noting that the hard subprocess in Fig. 3(b) is independent of $\ell_{1,2}^-$ and $\ell_{1,2\perp}$ we see that the target blob is described by a GPD, in analogy to the DVCS case of Fig. 1(c) discussed above,

$$\begin{aligned} T(\pi^+ N \rightarrow \gamma_L^* Y) &= \frac{-ieg^2 C_F}{2\pi Q \sqrt{2N_c}} \int dx C(x_B, x) \\ &\times \int dy_1^- e^{-iy_1^- \ell_1^+ / 2} \langle Y(p') | \bar{\psi}_u(y_1) \gamma^+ \gamma_5 \psi_d(0) | N(p) \rangle_{y_1^+ = y_{1\perp} = 0} \end{aligned} \quad (14)$$

where $x = \ell_1^+ / p^+$. The matrix element corresponds to a “transition” ($N \rightarrow Y$) GPD and the hard subprocess gives at lowest order

$$C(x_B, x) \equiv \int_0^1 dz \phi_\pi(z) \left(\frac{e_u}{1-z} \frac{1}{x_B + x + i\varepsilon} + \frac{e_d}{z} \frac{1}{x - i\varepsilon} \right) \quad (15)$$

The virtual photon is dominantly longitudinal for any state Y (we recall that $M_Y^2 \ll s$ according to (8)). In the case of $Y = N$ this is well-known from the time-reversed process $\gamma^* N \rightarrow \pi N$. The reason may more generally be understood as a consequence of the conservation of J^z and the suppression

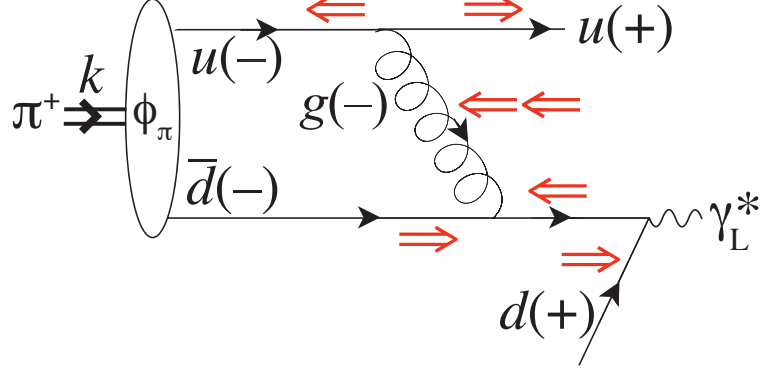


Fig. 4. The double red arrows indicate the spin directions of the particles. All momenta are in the $\pm z$ -direction as shown in the parentheses. The u -quark propagates into the GPD (not shown) while the d -quark propagates out of it.

of $L^z \sim q_\perp/Q$ due to the limited transverse momenta. In Fig. 4 the u -quark in the pion is taken to have helicity $+\frac{1}{2}$, hence $S_u^z = -\frac{1}{2}$ due to its large k_1^- (as indicated in parenthesis, the u -quark is moving in the $-z$ -direction). After emitting the gluon the u -quark has reversed its direction (more precisely, the hard process depends only on ℓ_1^+ in Fig. 3(b)). Since its helicity is conserved it now has $S_u^z = +\frac{1}{2}$. The gluon takes up the difference, $S_g^z = -1$ since $L_g^z = \mathcal{O}(1/Q)$. The \bar{d} quark in the pion has $S_{\bar{d}}^z = +\frac{1}{2}$ since $S_\pi^z = 0$. Helicity conservation then dictates that the target d -quark also has $S^z = \frac{1}{2}$ (\bar{d} and d have opposite helicity and move in opposite directions). After absorbing the gluon the \bar{d} has $S_{\bar{d}}^z = \frac{1}{2} - 1 = -\frac{1}{2}$, and the photon thus gets $S_{\gamma^*}^z = -\frac{1}{2} + \frac{1}{2} = 0$, *i.e.*, it is longitudinal. Since the \bar{d} quark virtuality is of $\mathcal{O}(Q^2)$ as it annihilates in the target its helicity and spin at that point are not simply related.

A corresponding analysis (as well as analytic calculation) shows [1] that the photon is transversely polarized in $pN \rightarrow \gamma^* Y$. In this case the Bj and BB limits give the same photon polarization, making it more difficult to distinguish the limits experimentally. The data on nucleon induced DY [7] shows the photon to be transversely polarized in the full measured range of x_F .

4. The inclusive $\pi^+ N \rightarrow \gamma^* Y$ cross section

The DY amplitudes (14) determine the inclusive cross section as

$$\sigma(\pi^+ N \rightarrow \gamma_L^* Y) = \frac{1}{2s} \sum_Y \int \frac{dq^- d^2 \mathbf{q}_\perp}{(2\pi)^3 2q^-} |T(\pi^+ N \rightarrow \gamma_L^* Y)|^2 (2\pi)^4 \delta^4(k+p-q-p') \quad (16)$$

The completeness sum

$$\sum_Y |Y\rangle \langle Y| \equiv \sum_{n=0}^{\infty} \int \prod_{i=1}^n \frac{d^3 \mathbf{p}_i}{(2\pi)^3 2E_i} |\mathbf{p}_1, \dots, \mathbf{p}_n\rangle \langle \mathbf{p}_1, \dots, \mathbf{p}_n| = 1 \quad (17)$$

requires an unlimited sum over all momenta \mathbf{p}_i and thus also over the total momentum $\mathbf{p}' = \sum_i \mathbf{p}_i$, which is constrained by the momentum-conserving δ -functions in (16). Before employing the closure relation we need to remove this explicit momentum constraint.

Integrating the inclusive cross section over the transverse momentum of the virtual photon eliminates the constraint on \mathbf{p}'_\perp . The longitudinal δ -functions may be expressed as Fourier integrals, and the p'^\pm -dependent phase incorporated in the matrix element using translation invariance:

$$\begin{aligned} & \int dy_3^+ dy_3^- \langle N(p) | \bar{\psi}_d(0) \gamma^+ \gamma_5 \psi_u(y_2) | Y(p') \rangle e^{iy_3 \cdot (k-q+p-p')} = \\ & = \int dy_3^+ dy_3^- \langle N(p) | \bar{\psi}_d(y_3) \gamma^+ \gamma_5 \psi_u(y_2 + y_3) | Y(p') \rangle e^{iy_3 \cdot (k-q)} \quad (18) \end{aligned}$$

The inclusive cross section is now seen to involve the multiparton distribution shown in Fig. 5,

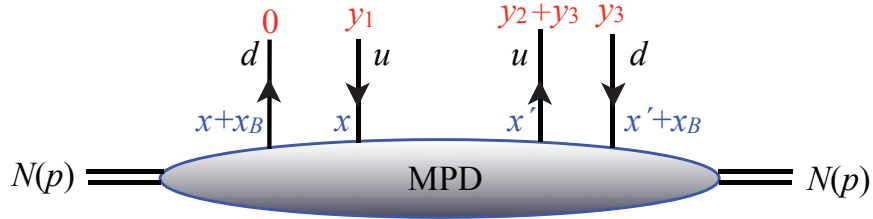


Fig. 5. Pictorial representation of the forward multiparton distribution $f_{d\bar{u}/p}(x_B, x_M; x, x')$ given in (19).

$$\begin{aligned} & f_{d\bar{u}/p}(x_B, x_M; x, x') = \quad (19) \\ & = \frac{1}{4(4\pi)^3} \int dy_1^- dy_2^- dy_3^- dy_3^+ \exp \left\{ \frac{1}{2} i \left[-y_1^- l_1^+ + y_2^- l_1^{+'} - y_3^- q^+ + y_3^+ x_M p^- \right] \right\} \\ & \quad \times \langle N(p) | \bar{\psi}_d(y_3) \gamma^+ \gamma_5 \psi_u(y_2 + y_3) \bar{\psi}_u(y_1) \gamma^+ \gamma_5 \psi_d(0) | N(p) \rangle_{y_{i\perp}=0; y_1^+=y_2^+=0} \end{aligned}$$

where $x' = \ell_1^+ / p^+$ and

$$x_M = \frac{k^-(1 - x_F)}{p^-} \quad (20)$$

is the ‘-’ momentum fraction of the pion (carried by the stopped quark in Fig. 3) which is transmitted into the inclusive system Y and determines its mass,

$$M_Y^2 = m_N^2(1 - x_B)(1 + x_M) - \mathbf{q}_\perp^2 \quad (21)$$

The constraint $M_Y \geq m_N$ implies

$$\frac{x_B + \mathbf{q}_\perp^2 / m_N^2}{1 - x_B} \leq x_M \leq \infty \quad (22)$$

In the BB limit M_Y and hence x_M are finite, and so is the conjugate variable, the LF time difference y_3^+ between the amplitudes T and T^\dagger .

The target matrix element is evaluated at both $y_3^+ > 0$ and $y_3^+ < 0$ in the MPD (19), and is thus not LF time ordered. However, for $y_3^+ < 0$ the order of the T and T^\dagger operators may be reversed by taking the hermitian conjugate of the matrix element. Hence the MPD may be expressed as the discontinuity of an LF time ordered matrix element, as expected from unitarity and indicated in Fig. 1(d). In this respect it differs from the multiparton distributions studied by Jaffe [8], which give higher twist corrections to hard processes in the standard Bj limit. Those distributions are real, since all operators are evaluated at equal LF time.

Including the hard subprocess amplitudes the $\pi^+ N \rightarrow \gamma^* Y$ cross section in the BB limit is

$$\begin{aligned} \frac{d\sigma(\pi^+ N \rightarrow \gamma_L^* Y)}{dM_Y^2} &= \quad (23) \\ &= \frac{2(e g^2 C_F)^2}{Q^2 s^2 (1 - x_B) N_c} \int dx dx' C(x_B, x) C^*(x_B, x') f_{d\bar{u}/p}(x_B, x_M; x, x') \end{aligned}$$

with $C(x_B, x)$ given in (15).

5. Reduction to incoherent jet production

We have considered the BB limit (4) of the DY process in which M_Y^2 (8) is fixed as $Q^2 \rightarrow \infty$. There was no restriction on the magnitude of M_Y^2 . According to (21) the momentum $k^-(1 - x_F) = x_M p^-$ of the ‘stopped’ quark in Fig. 3 grows with M_Y^2 and can become large enough for the quark to hadronize independently of the target spectators (Fig. 6), as in the standard

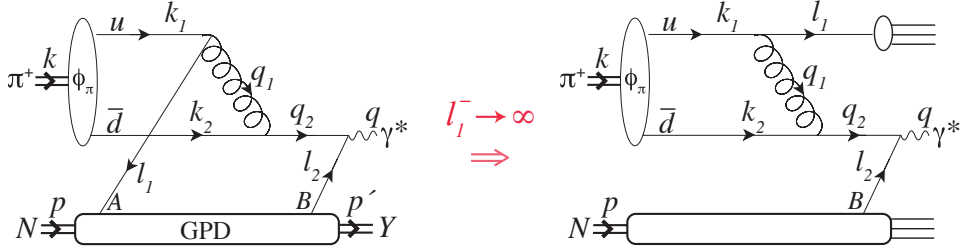


Fig. 6. In the secondary limit where the stopped u -quark momentum ℓ_1^- (and hence also M_Y) is large, the quark hadronizes independently of the target spectators (right). Squaring and summing the amplitudes turns the target matrix element into a d -quark PDF as in (24).

Bj limit. Thus for large M_Y^2 the MPD target matrix element (19) should reduce to a standard target PDF. This may indeed be verified as follows.

At large $x_M p^-$ the conjugate LF time vanishes, $y_3^+ \rightarrow 0$ in the MPD expression (19). If we take the u -quark to be the stopped one as in Fig. 3, $\ell_1^- = x_M p^-$ is large and $\ell_1^+ \propto 1/x_M p^- \rightarrow 0$ in order that the u -quark remain close to on-shell. The u -quark propagation becomes light-cone dominated and the contraction of the fields $\psi_u(y_2 + y_3)\bar{\psi}_u(y_1)$ may be approximated by the free propagator. We find [1]

$$f_{d\bar{u}/p}(x_B, x_M; x, x') \rightarrow \frac{1}{4\pi} \delta(x - x') \theta(x) f_{d/p}(x_B) \quad (\ell_1^- \rightarrow \infty) \quad (24)$$

The expression for the DY cross section in the BB limit at large M_Y is then equivalent to the one obtained in [6],

$$\frac{d\sigma(\pi^+ N \rightarrow \gamma_L^* Y)}{dM_Y^2} = \frac{(e e_d g^2 C_F)^2}{Q^2 s^2 (1 - x_B) N_c} \int \frac{dx}{2\pi x} \theta(x) \left(\int \frac{dz}{z} \phi_\pi(z) \right)^2 f_{d/p}(x_B) \quad (25)$$

6. Summary

The BB limit (4), $Q^2 \rightarrow \infty$ at fixed $(1 - x_B)Q^2$, is not compatible with factorization at leading twist in DIS, $eN \rightarrow eX$. Coherence of the struck quark with the target remnant cannot be neglected at finite M_X as is evident from the limiting case of $x_B = 1$ ($eN \rightarrow eN$). Nevertheless, the success of Bloom-Gilman duality [2] indicates that both the Bj limit ($M_X \rightarrow \infty$) and the BB limit ($M_X = M_{N^*}$ fixed) are relevant for $eN \rightarrow eN^*$ (elastic and transition form factors).

The BB limit is appropriate for describing factorization in hard exclusive processes such as DVCS, $\gamma^* N \rightarrow \gamma(x_F)Y$, since a fixed mass M_Y implies

fixed $(1 - x_F)Q^2$ (*cf.* (8)). The coherence effects between the struck quark (which stops in the target after emitting the photon) and the target remnants are then described by the GPD.

We may use completeness in the system Y to relate the cross section of the *inclusive* DVCS process $\sum_Y \sigma(\gamma^*N \rightarrow \gamma Y)$ to the discontinuity of a forward multiparton distribution (Fig. 1(d)). This applies to many other hard inclusive processes as well and offers novel opportunities to relate measurable cross sections to precisely defined target matrix elements.

We studied in detail the BB limit of the DY process $\pi N \rightarrow \gamma^*(x_F)Y$. This offers a possibility to estimate how high x_F needs to be (or equivalently, how low the inclusive mass M_Y) for the BB limit to apply. In the Bj limit (x_F fixed, $M_Y \rightarrow \infty$) the γ^* is transversely polarized, whereas it is longitudinal in the BB limit ($x_F \rightarrow 1$, M_Y fixed). For $Q^2 > 16 \text{ GeV}^2$ the transition was found [5] to start at $x_F \gtrsim 0.6$, with the γ^* being dominantly longitudinal at $x_F = 0.9$ ($M_Y \simeq 7 \text{ GeV}$). In nucleon induced DY, $NN \rightarrow \gamma^*(x_F) + Y$, the γ^* is predicted [1] to be transversely polarized in both the Bj and BB limits. The available data [7] indeed shows no polarization change as a function of x_F .

The large Single Spin Asymmetries (SSA) observed at high x_F in $p^\uparrow p \rightarrow \pi + Y$ [9] and $pp \rightarrow \Lambda^\uparrow + Y$ [10] suggest another application of BB dynamics [11]. The SSA requires both helicity flip and a dynamic phase, both of which are suppressed in hard subprocesses. In the BB limit the helicity flip may occur in a *soft* interaction of a low- x parton which is coherent with the hard process producing the hadron with high x_F and p_\perp . This may explain the very large asymmetries observed as well as the puzzling fact that the asymmetry appears not to decrease with p_\perp , as expected in the standard leading twist framework.

Acknowledgements I am grateful to the Organizers for their invitation to this meeting dedicated to the memory of Jan Kwieciński, a close friend and collaborator of mine. The work described in this talk is based on my collaboration with Matti Järvinen and Samu Kurki. Travel support by the Magnus Ehrnrooth Foundation is gratefully acknowledged.

REFERENCES

- [1] P. Hoyer, M. Järvinen and S. Kurki, JHEP **0810** (2008) 086 [arXiv:0808.0626 [hep-ph]].
- [2] W. Melnitchouk, R. Ent and C. Keppel, Phys. Rept. **406** (2005) 127 [arXiv:hep-ph/0501217];

- Proceedings, 1st Workshop on Quark-Hadron Duality and the Transition to pQCD, Frascati 2005 (World Scientific, 2006; ISBN 981-256-684-8) <http://www.lnf.infn.it/conference/duality05/>
- [3] P. Hoyer, *Inclusive Perspectives*, Concluding talk at the Workshop on Exclusive Reactions at High Momentum Transfer, Jefferson Lab (May 2007). Published in the Proceedings (World Scientific, 2008, ISBN-10 981-279-694-0, p. 55) [arXiv:0708.2808 [hep-ph]].
 - [4] M. Diehl, Phys. Rept. **388** (2003) 41 [arXiv:hep-ph/0307382].
 - [5] K. J. Anderson *et al.*, Phys. Rev. Lett. **43** (1979) 1219;
J. P. Alexander *et al.*, Phys. Rev. D **34** (1986) 315;
J. G. Heinrich *et al.*, Phys. Rev. D **44** (1991) 1909.
 - [6] E. L. Berger and S. J. Brodsky, Phys. Rev. Lett. **42** (1979) 940;
E. L. Berger, Phys. Lett. B **89** (1980) 241.
 - [7] L. Y. Zhu *et al.* [FNAL-E866/NuSea Collaboration], Phys. Rev. Lett. **99** (2007) 082301 [arXiv:hep-ex/0609005];
P. L. McGaughey, J. M. Moss and J. C. Peng, Ann. Rev. Nucl. Part. Sci. **49** (1999) 217 [arXiv:hep-ph/9905409];
L. Y. Zhu *et al.* [FNAL E866/NuSea Collaboration], arXiv:0811.4589 [nucl-ex] and J. C. Peng, private communication.
 - [8] R. L. Jaffe, Nucl. Phys. B **229** (1983) 205.
 - [9] D. L. Adams *et al.* [E581 Collaboration], Phys. Lett. B **261** (1991) 201;
D. L. Adams *et al.* [FNAL-E704 Collaboration], Phys. Lett. B **264** (1991) 462;
A. Bravar *et al.* [Fermilab E704 Collaboration], Phys. Rev. Lett. **77** (1996) 2626;
J. Adams *et al.* [STAR Collaboration], Phys. Rev. Lett. **92** (2004) 171801 [arXiv:hep-ex/0310058].
 - [10] G. Bunce *et al.*, Phys. Rev. Lett. **36** (1976) 1113;
K. J. Heller *et al.*, Phys. Lett. B **68** (1977) 480;
B. Lundberg *et al.*, Phys. Rev. D **40** (1989) 3557;
A. Bravar *et al.* [E704 Collaboration], Phys. Rev. Lett. **75** (1995) 3073;
A. Bravar *et al.* [E704 Collaboration], Phys. Rev. Lett. **78** (1997) 4003.
 - [11] P. Hoyer and M. Järvinen, JHEP **0702** (2007) 039 [arXiv:hep-ph/0611293].